

# Chaotic synchronization of two optical cavity modes in optomechanical systems

Nan Yang,<sup>1,2,\*</sup> Adam Miranowicz,<sup>1,3</sup> Yong-Chun Liu,<sup>4</sup> Keyu Xia,<sup>2,5,1,†</sup> and Franco Nori<sup>1,6</sup>

<sup>1</sup>*CEMS, RIKEN, Saitama, 351-0198, Japan*

<sup>2</sup>*National Laboratory of Solid State Microstructures, College of Engineering and Applied Sciences, Nanjing University, Nanjing, 210093, China*

<sup>3</sup>*Faculty of Physics, Adam Mickiewicz University, 61-614 Poznan, Poland*

<sup>4</sup>*State Key Laboratory of Low Dimensional Quantum Physics and Department of Physics, Tsinghua University, Beijing, 100084, China*

<sup>5</sup>*Collaborative Innovation Center of Advanced Microstructures, Nanjing 210093, China*

<sup>6</sup>*Physics Department, The University of Michigan, Ann Arbor, Michigan 48109-1040, USA*

(Dated: February 12, 2018)

The synchronization of the motion of microresonators has attracted considerable attention. Here we present theoretical methods to synchronize the chaotic motion of two optical cavity modes in an optomechanical system, in which one of the optical modes is strongly driven into chaotic motion and is coupled to another weakly-driven optical mode mediated by a mechanical resonator. In these optomechanical systems, we can obtain both complete and phase synchronization of the optical cavity modes in chaotic motion, starting from different initial states. We find that complete synchronization of chaos can be achieved in two identical cavity modes. In the strong-coupling small-detuning regime, we also produce phase synchronization of chaos between two nonidentical cavity modes.

## I. INTRODUCTION

The synchronization of oscillators is a universal concept in nonlinear sciences [1, 2]. It has been observed in both nature [2] and social activities [1–3], and also promises important applications in engineering [1, 2, 4–6]. Since its discovery in pendulum systems by Huygens in the 17th century [7], synchronization has been observed in various fields including bursting neurons [8], fireflies [9], and chemical reactions [10]. Although these systems operate in very different size scales, the mechanism behind synchronization can be understood as follows: oscillators under weak interaction adjust their rhythms to keep their motions consistent. The synchronization of oscillators has been studied in relation to information processing [4], communications [5], and high-precision clocks [6].

Optomechanical resonators [11–24] with high-quality factors and strong nonlinearities have attracted considerable attention in various fields due to their promising applications. The synchronization of optomechanical systems is an important topic in optomechanics [25–34]. However, the majority of previous works concentrate on the synchronization of *periodic* oscillations. The *chaotic* synchronization [35] of an optomechanical system is very challenging because chaotic signals are extremely sensitive to initial conditions. It is still an open question whether microscopic optomechanical systems with chaotic motion can be synchronized. Optomechanical systems with strong nonlinear light-matter interactions can support quite different types of motion, i.e., periodic [12], quasi-periodic [21], and chaotic [19–24]. Thus, the study of chaotic synchronization of optomechanical systems may provide an answer to this question.

In this paper, we study both complete and phase synchronization of two optical cavity modes in an optomechanical

system with chaotic dynamics rather than with periodic motion. We consider an optical cavity mode strongly driven to a chaotic state. This brings other weakly-driven optical-cavity modes into chaos mediated by a mechanical motion [21]. Thus, it is found that complete synchronization is achievable in two identical weakly-driven cavity modes, and phase synchronization can be realized in the strongly- and weakly-driven cavity modes, although these two optical modes are initially in different states.

The active-passive decomposition (APD) model [36, 37] is widely used to describe systems in complete synchronization. In the APD model, different subsystems under a common driving force can achieve complete synchronization regardless of their initial conditions. This APD model can also describe our chaotic system. The complete synchronization studied here (as shown in Fig. 1) involves three cavity modes coupled to a common mechanical oscillator in an optomechanical system. One of the cavity modes,  $\hat{a}_s$ , is strongly driven into chaotic motion. Mediated by the mechanical oscillation, it also drives the other two weakly-driven optical cavity modes,  $\hat{a}_1$  and  $\hat{a}_2$ , into chaotic motion. We show that this chaotic motion of the modes  $\hat{a}_1$  and  $\hat{a}_2$  can be completely synchronized. However, this complete synchronization can only be realized in identical chaotic systems. A small mismatch in design of two synchronized subsystems can destroy their complete synchronized behavior.

In contrast to complete synchronization, phase synchronization can be realized between two nonidentical chaotic systems through interacting with a common mechanical motion (see Fig. 2). To achieve such phase synchronization, one optical cavity mode ( $\hat{a}_s$ ) in the optomechanical system is strongly driven by an external classical field, while the other mode ( $\hat{a}_w$ ) is weakly driven. Phase synchronization of the optical modes can be achieved when the cavity-driving detuning is much smaller than the optomechanical coupling. We find that the temporal phases of the two optical modes with chaotic motion mainly depend on the mechanical displacement, which is governed by the cavity mode  $\hat{a}_s$ . Thus, although the two optical

\* nan.yang@riken.jp

† keyu.xia@nju.edu.cn

modes are in chaotic motion, their unwrapped phases can be locked to each other at a fixed ratio. In the following, we investigate these two kinds of synchronization in two different models.

We propose two setups (A and B) for either complete synchronization or phase synchronization of the optical modes in an optomechanical system. Both setups A and B share a common configuration: the strongly-driven cavity mode  $\hat{a}_s$  dominates the motion of the weakly-driven cavity modes. In setup A, the strongly- and weakly-driven cavity modes are coupled via a mechanical mode, while they are coupled via two mechanical resonators in setup B. In comparison with the setup A, a strong coupling between two mechanical resonators is required in setup B.

This paper is organized as follows: In Secs. II and III, we present the corresponding setups for both complete and phase synchronization in an optomechanical system. The numerical results for these two types of synchronization are shown and compared in Sec. IV. In Sec. V, we summarize our work and discuss some potential applications.

## II. COMPLETE SYNCHRONIZATION

In this section, we focus on the complete synchronization of an optomechanical system. In general terms, complete synchronization refers to the identity among the phase-space orbits of chaotic systems. Let us consider two chaotic systems

$$\dot{\mathbf{y}}_1 = \mathbf{f}(\mathbf{y}_1), \quad \dot{\mathbf{y}}_2 = \mathbf{f}(\mathbf{y}_2), \quad (1)$$

where  $\mathbf{y}_1$  and  $\mathbf{y}_2$  are  $N$ -dimensional variables governed by the function  $\mathbf{f} : R^N \rightarrow R^N$ . We define the difference between the phase-space orbits of two chaotic systems as the synchronization error  $\mathbf{e}(t)$ , where  $\mathbf{e}(t) = \mathbf{y}_1(t) - \mathbf{y}_2(t)$ . Two chaotic systems are called completely synchronized if and only if their synchronization error  $\mathbf{e}(t)$  vanishes in the evolution long time limit [38], i.e.,

$$\lim_{t \rightarrow \infty} \mathbf{e}(t) = \lim_{t \rightarrow \infty} \|\mathbf{y}_1(t) - \mathbf{y}_2(t)\| = 0. \quad (2)$$

The drive-response model [38] and the active-passive decomposition (APD) model [36, 37] are two widely used methods for characterizing the complete synchronization of chaotic systems. In the former model, the drive and response systems, which are to be synchronized, are in the unidirectional-coupling regime. It is required that the response system can be decomposed into a stable subsystem and an unstable one. By controlling the motion of the unstable subsystem, the driving part can force the phase-space orbit of the response part to reach a synchronized state. However, the drive-response model can only be applied to decomposable chaotic systems. This seriously restricts its applications in engineering. The APD model, as an advanced version of the drive-response model, provides a more general way to study complete synchronization. In the APD model, two chaotic parts to be synchronized can be written as the nonautonomous form:

$$\dot{\mathbf{z}}_1 = \mathbf{g}[\mathbf{z}_1, \mathbf{s}(t)], \quad \dot{\mathbf{z}}_2 = \mathbf{g}[\mathbf{z}_2, \mathbf{s}(t)], \quad (3)$$

where the temporal evolutions of  $\mathbf{z}_1$  and  $\mathbf{z}_2$  are ruled by the function  $\mathbf{g}$ , and  $\mathbf{s}(t)$  is the common external driving governed by the autonomous function  $\dot{\mathbf{s}}(t) = \mathbf{h}[\mathbf{s}(t)]$ . The APD model provides a flexible method to find a proper function  $\mathbf{h}[\mathbf{s}(t)]$  for the complete synchronization of chaotic systems. In this section, we use the APD model to study the chaotic synchronization of the two optical cavity modes in an optomechanical system.

According to the APD model, we propose two setups for realizing the complete synchronization of chaotic optical modes in an optomechanical system (see Fig. 1). It can be seen that both setups consist of three subsystems: (i) a strongly-driven cavity mode,  $\hat{a}_s$ ; (ii) two weakly-driven cavity modes,  $\hat{a}_1$  and  $\hat{a}_2$ ; (iii) mechanical mode(s), either  $b$  in setup A, or  $\hat{b}_s, \hat{b}_1$ , and  $\hat{b}_2$  in setup B. Here, the cavity mode  $\hat{a}_s$  is strongly driven to induce chaos. This chaos can be then transferred to the two weakly-driven cavity modes ( $\hat{a}_1$  and  $\hat{a}_2$ ) via the mechanical resonator(s) [21]. In the APD model, the mechanical oscillation corresponds to an external signal and the weakly-driven cavity modes are the two subsystems to be synchronized. We show that under the common driving of the chaotic mechanical resonator, the two weakly-driven optical modes can be excited to chaotic states (see Fig. 3) and can evolve into a completely-synchronized state (see Fig. 4). For simplicity, we neglect both thermal noise and quantum noise. This is valid under the following assumptions: (i) the thermal occupation of the cooled mechanical resonators is low, such that the thermal noise of the mechanical oscillators is small in comparison with the motion caused by the applied driving; (ii) the optomechanical system is driven by strong laser fields and, therefore, can be treated as a classical system. Under these conditions, the effect of environmental thermal noise and quantum noise of our optomechanical system can be neglected.

### A. Complete synchronization in setup A

We start our discussion of complete synchronization by introducing setup A, shown in Fig. 1(a). One strongly and two weakly-driven cavity modes are coupled to the same mechanical mode. Here the strongly-driven optical mode creates mechanical chaos through nonlinear optomechanical coupling. In this arrangement, the fields in the weakly-driven cavity modes are modulated in a chaotic way by the chaotic mechanical mode. The total Hamiltonian of this synchronized system is given by (we set  $\hbar = 1$  and always assume  $j = 1, 2$ ):

$$\begin{aligned} \hat{H} = & \Delta_s \hat{a}_s^\dagger \hat{a}_s + \sum_j \Delta_j \hat{a}_j^\dagger \hat{a}_j + \Omega_m \hat{b}^\dagger \hat{b} \\ & + i\varepsilon_s (\hat{a}_s^\dagger - \hat{a}_s) + i \sum_j \varepsilon_j (\hat{a}_j^\dagger - \hat{a}_j) \\ & + g_s \hat{a}_s^\dagger \hat{a}_s (\hat{b} + \hat{b}^\dagger) + \sum_j g_j \hat{a}_j^\dagger \hat{a}_j (\hat{b} + \hat{b}^\dagger), \end{aligned} \quad (4)$$

where  $\hat{a}_s$  ( $\hat{a}_j$ ) denotes the annihilation operator of the strongly (weakly) driven cavity mode,  $\Delta_s = \omega_{\text{cav},s} - \omega_{d,s}$  ( $\Delta_j = \omega_{\text{cav},j} - \omega_{d,j}$ ) stands for the corresponding detuning between the cavity resonance frequency  $\omega_{\text{cav},s}$  ( $\omega_{\text{cav},j}$ ) and the input laser fre-

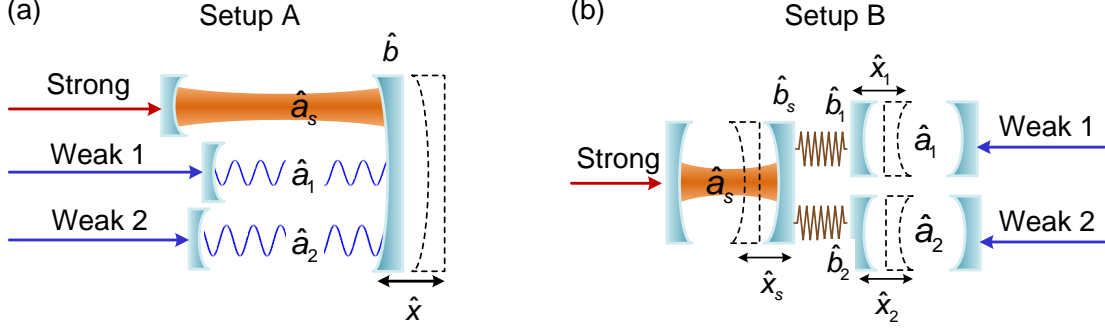


FIG. 1. (Color online) Schematic diagrams of two optomechanical models for complete synchronization. (a) Setup A includes a strongly-driven cavity mode  $\hat{a}_s$ , two weakly-driven cavity modes  $\hat{a}_j$ , and a mechanical mode  $b$ . The strongly- and weakly-driven cavity modes are coupled via the mechanical mode with coupling strengths  $g_s$  and  $g_j$ , respectively. (b) Setup B consists of a strongly-driven cavity mode  $\hat{a}_s$  and two weakly-driven cavity modes  $\hat{a}_j$ , where the latter are coupled to  $\hat{a}_s$  via the mechanical modes  $b_j$  and  $b_s$ , which are additionally coupled to each other with the spring coefficients  $k_j$ .

quency  $\omega_{d,s}$  ( $\omega_{d,j}$ ), and  $\varepsilon_s$  ( $\varepsilon_j$ ) is the driving strength of the cavity mode  $\hat{a}_s$  ( $\hat{a}_j$ ). The annihilation operator of the mechanical resonator is represented by  $\hat{b}$ , and  $\Omega_m$  denotes its natural frequency. Here,  $g_s$  ( $g_j$ ) is the optomechanical single-photon coupling strength between the cavity mode  $\hat{a}_s$  ( $\hat{a}_j$ ) and the mechanical mode  $\hat{b}$ .

To obtain the equation of motion of the system in the classical regime, we first write the quantum Langevin equations for the Hamiltonian, given in Eq. (4), as:

$$\dot{\hat{a}}_s = -i\Delta_s \hat{a}_s - \frac{\gamma_s}{2} \hat{a}_s - ig_s \hat{a}_s (\hat{b}^\dagger + \hat{b}) + \varepsilon_s, \quad (5a)$$

$$\dot{\hat{b}} = -i\Omega_m \hat{b} - \frac{\Gamma_m}{2} \hat{b} - ig_s \hat{a}_s^\dagger \hat{a}_s - ig_j \hat{a}_j^\dagger \hat{a}_j, \quad (5b)$$

$$\dot{\hat{a}}_j = -i\Delta_j \hat{a}_j - \frac{\gamma_j}{2} \hat{a}_j - ig_j \hat{a}_j (\hat{b}^\dagger + \hat{b}) + \varepsilon_j, \quad (5c)$$

where  $\gamma_s$  ( $\gamma_j$ ) and  $\Gamma_m$  are the damping rates of the cavity mode  $\hat{a}_s$  ( $\hat{a}_j$ ) and the mechanical mode  $\hat{b}$ , respectively.

We treat the optomechanical device as a classical system such that we can replace the quantum operators with their classical mean values:  $\alpha_s = \langle \hat{a}_s \rangle$ ,  $\alpha_j = \langle \hat{a}_j \rangle$ , and  $\beta = \langle \hat{b} \rangle$ . Note that the thermal noise and quantum noise are neglected, as explained above. In this configuration,  $\alpha_j$  are the two classical cavity modes to be synchronized, which are governed by

$$\dot{\alpha}_j = -i\Delta_j \alpha_j - \frac{\gamma_j}{2} \alpha_j - iG_j \alpha_j x + \varepsilon_j, \quad (6)$$

where  $x = x_{\text{ZPF}}(\beta + \beta^*)$  refers to the classical mechanical displacement, and its nonlinear coupling strength with the optical mode  $\alpha_j$  is denoted by  $G_j = g_j/x_{\text{ZPF}}$ . Here  $x_{\text{ZPF}}$  is the zero-point fluctuation (ZPF) displacement of the mechanical resonator.

We apply the drivings in a way that the radiation pressure of the weakly-driven cavity modes  $\alpha_1$  and  $\alpha_2$  on the mechanical mode  $\beta$  is negligibly weak in comparison with that caused by the strongly-driven cavity mode  $\alpha_s$ . In this arrangement, the mechanical displacement  $x$  is dominantly determined by the strongly-driven optical mode. It subsequently governs the motion of the weakly-driven cavity modes  $\alpha_j$  by modulating their

resonance frequencies. The back-action from the cavity mode  $\alpha_j$  on  $x$  can be neglected. We denote this as the unidirectional-coupling regime, in which the force of the weakly-driven cavity modes  $\alpha_1$  and  $\alpha_2$  acting on the mechanical resonator can be neglected. The mechanical displacement  $x$ , as an external signal, modulates these two cavity modes  $\alpha_1$  and  $\alpha_2$  in the same way. As a result, the chaotic synchronization of the two weakly-driven cavity modes  $\alpha_1$  and  $\alpha_2$  can be obtained.

In this unidirectional-coupling regime, the motion of the cavity mode  $a_s$  and the mechanical resonator are reduced to

$$\dot{\alpha}_s = -i\Delta_s \alpha_s - \frac{\gamma_s}{2} \alpha_s - iG_s \alpha_s x + \varepsilon_s, \quad (7a)$$

$$m_{\text{eff}} \ddot{x} = -m_{\text{eff}} \Omega_m^2 x - m_{\text{eff}} \Gamma_m \dot{x} + \hbar G_s |\alpha_s|^2, \quad (7b)$$

where  $m_{\text{eff}}$  denotes the effective mass of the mechanical resonator. This configuration can be understood in the APD model as follows: The two identical cavity modes  $\alpha_1$  and  $\alpha_2$  are two subsystems to be synchronized. The mechanical displacement  $x$  produces a common external force on these two modes. These two cavity modes are asymptotically stable. The configuration satisfies the necessary conditions for their complete synchronization.

## B. Complete synchronization in setup B

In this subsection, we focus on setup B shown in Fig. 1(b). Specifically, this system consists of one strongly and two weakly-driven optomechanical systems, each of which includes only a single cavity mode and a mechanical mode. Different from setup A, here the optomechanical systems are coupled with each other via the mechanical resonators: each mechanical mode  $b_j$  in the weakly-driven optomechanical system is coupled to the mechanical mode  $b_s$  in the strongly-driven optomechanical system with a coupling coefficient  $k_j$ . The

total Hamiltonian of this system is described by

$$\begin{aligned} \hat{H} = & \Delta_s \hat{a}_s^\dagger \hat{a}_s + \Delta_j \hat{a}_j^\dagger \hat{a}_j + \Omega_s \hat{b}_s^\dagger \hat{b}_s + \sum_j \Omega_j \hat{b}_j^\dagger \hat{b}_j \\ & + g_s \hat{a}_s^\dagger \hat{a}_s (\hat{b} + \hat{b}^\dagger) + \sum_j g_j \hat{a}_j^\dagger \hat{a}_j (\hat{b}_j + \hat{b}_j^\dagger) \\ & + \sum_j k_j (\hat{b}_j^\dagger + \hat{b}_j) (\hat{b}_s + \hat{b}_s^\dagger) + i \varepsilon_s (\hat{a}_s^\dagger - \hat{a}_s) \\ & + i \sum_j \varepsilon_j (\hat{a}_j^\dagger - \hat{a}_j), \end{aligned} \quad (8)$$

where  $\hat{a}_s$  ( $\hat{a}_j$ ) refers to the annihilation operator of the cavity mode in the strongly (weakly) driven optomechanical system,  $\Delta_s$  ( $\Delta_j$ ) and  $\varepsilon_s$  ( $\varepsilon_j$ ) are the corresponding detuning and driving strength, respectively. Here,  $\hat{b}_s$  ( $\hat{b}_j$ ) is the annihilation operator of the mechanical mode in the strongly (weakly) driven optomechanical system and its resonance frequency is denoted as  $\Omega_s$  ( $\Omega_j$ ); while  $g_s$  ( $g_j$ ) is the optomechanical single-photon coupling strength between the cavity mode  $\hat{a}_s$  ( $\hat{a}_j$ ) and the mechanical mode  $\hat{b}_s$  ( $\hat{b}_j$ ), and  $k_j$  denotes the coupling strength between the mechanical modes  $\hat{b}_j$  and  $\hat{b}_s$ . Because identical subsystems are required to achieve their complete synchronization, the coupling coefficients are set to be the same,  $k_1 = k_2$ . From the Hamiltonian, given in Eq. (8), we have the following quantum Langevin equations:

$$\dot{\hat{a}}_s = -i\Delta_s \hat{a}_s - \frac{\gamma_s}{2} \hat{a}_s - ig_s \hat{a}_s (\hat{b}_s^\dagger + \hat{b}_s) + \varepsilon_s, \quad (9a)$$

$$\dot{\hat{b}}_s = -i\Omega_s \hat{b}_s - \frac{\Gamma_s}{2} \hat{b}_s - ig_s \hat{a}_s^\dagger \hat{a}_s, \quad (9b)$$

$$\dot{\hat{a}}_j = -i\Delta_j \hat{a}_j - \frac{\gamma_j}{2} \hat{a}_j - ig_j \hat{a}_j (\hat{b}_j^\dagger + \hat{b}_j) + \varepsilon_j, \quad (9c)$$

$$\dot{\hat{b}}_j = -i\Omega_j \hat{b}_j - \frac{\Gamma_j}{2} \hat{b}_j - ig_j \hat{a}_j^\dagger \hat{a}_j + ik_j (\hat{b}_s + \hat{b}_s^\dagger), \quad (9d)$$

where  $\gamma_s$  ( $\gamma_j$ ) and  $\Gamma_s$  ( $\Gamma_j$ ) refer to the damping rates of the optical mode  $\hat{a}_s$  ( $\hat{a}_j$ ) and the mechanical mode  $\hat{b}_s$  ( $\hat{b}_j$ ) in the strongly (weakly) driven optomechanical system. Let  $\alpha_s$ ,  $\alpha_j$ ,  $\beta_s$ , and  $\beta_j$  be the mean values of  $\hat{a}_s$ ,  $\hat{a}_j$ ,  $\hat{b}_s$ , and  $\hat{b}_j$ :  $\alpha_s = \langle \hat{a}_s \rangle$ ,  $\alpha_j = \langle \hat{a}_j \rangle$ ,  $\beta_s = \langle \hat{b}_s \rangle$ , and  $\beta_j = \langle \hat{b}_j \rangle$ . In the semiclassical regime, the operators  $\hat{a}_s$ ,  $\hat{a}_j$ ,  $\hat{b}_s$ , and  $\hat{b}_j$  in Eq. (9) can be replaced by classical variables  $\alpha_s$ ,  $\alpha_j$ ,  $\beta_s$ , and  $\beta_j$ . Here, the two classical weakly-driven optomechanical systems to be synchronized are governed by:

$$\dot{\alpha}_j = -i\Delta_j \alpha_j - \frac{\gamma_j}{2} \alpha_j + iG_j \alpha_j x_j + \varepsilon_j, \quad (10a)$$

$$\begin{aligned} m_{\text{meff},j} \ddot{x}_j = & -m_{\text{meff},j} \Omega_j^2 x_j - m_{\text{meff},j} \Gamma_j \dot{x}_j + \hbar G_j |\alpha_j|^2 \\ & - K_j (x_j - x_s). \end{aligned} \quad (10b)$$

These two systems, described in Eq. (10), are driven by the same strongly-driven optomechanical system:

$$\dot{\alpha}_s = -i\Delta_s \alpha_s - \frac{\gamma_s}{2} \alpha_s - iG_s \alpha_s x_s + \varepsilon_s, \quad (11a)$$

$$m_{\text{meff},s} \ddot{x}_s = -m_{\text{meff},s} \Omega_s^2 x_s - m_{\text{meff},s} \Gamma_s \dot{x}_s + \hbar G_s |\alpha_s|^2, \quad (11b)$$

where  $m_{\text{meff},s}$  ( $m_{\text{meff},j}$ ),  $x_s$  ( $x_j$ ), and  $G_s$  ( $G_j$ ) are the mechanical effective mass, mechanical displacement, and the optical-mechanical coupling strength of the strongly (weakly) driven

optomechanical resonator, respectively. Here,  $x_s$  ( $x_j$ ) is defined as  $x_s = x_{\text{ZPF}}^s (\beta_s + \beta_s^*)$  [ $x_j = x_{\text{ZPF}}^j (\beta_j + \beta_j^*)$ ], and we define  $G_s = g_s / x_{\text{ZPF}}^s$  ( $G_j = g_j / x_{\text{ZPF}}^j$ ), where  $x_{\text{ZPF}}^s$  ( $x_{\text{ZPF}}^j$ ) is the ZPF of the strongly (weakly) driven optomechanical resonators. The external force acting on the mechanical resonator associated with the displacement  $x_j$  takes the form  $-K_j (x_j - x_s)$ , where  $K_j = \hbar k_j / (x_{\text{ZPF}}^s x_{\text{ZPF}}^j)$  is the classical mechanical coupling strength. When  $K_1 / m_{\text{eff},1} = K_2 / m_{\text{eff},2}$ , the two weakly-driven modes share the same dynamics. Thus, this system can be studied in the framework of the APD configuration: two weakly-driven optomechanical resonators as two chaotic subsystems are synchronized and the strongly-driven optomechanical resonator acts as a common external force.

Note that the external-force term  $-K_j (x_j - x_s)$  in Eq. (11b) is derived from the classical Lagrangian  $L_{\text{int}} = K_j (x_j - x_s)^2 / 2$ . If we start from the quantum Langevin equations, shown in Eq. (9d), then the external-force term should be  $K_j x_s$ . This difference  $-K_j x_j$  between these two functions originates from the quantization of classical coupled-spring oscillators. Quantum systems interact with each other in the discontinuous regime, while the classical ones interact in the continuous regime. When  $\Omega_j^2 \gg K_j$ , the term  $-K_j x_j$  in Eq. (10b) is very small when compared to other terms and can be omitted. Thus, Eqs. (9d) and (10b) are consistent for high-frequency resonators.

### III. PHASE SYNCHRONIZATION

In Sec. II, we discussed the complete synchronization of two identical chaotic optical modes in optomechanical systems. However, it is technically challenging to fabricate two identical optomechanical resonators. Even a tiny parameter mismatch between two chaotic optomechanical resonators can destroy their complete synchronization. Thus, the research of synchronization in nonidentical chaotic systems is of importance. So far, there are many attempts for synchronization of two nonidentical chaotic systems, including phase synchronization [39, 40], generalized synchronization [41, 42], and time-delayed synchronization [43]. In this section, we show that the phases of two nonidentical chaotic cavity modes can be locked at a fixed ratio, although their amplitudes are irrelevant to each other.

In general, two periodic systems are called phase synchronized if their phases  $\psi_1(t)$  and  $\psi_2(t)$  are locked at a fixed ratio  $m/n$ , i.e.,  $|n\psi_1(t) - m\psi_2(t)| < \text{constant}$ , where  $m$  and  $n$  are integers. Recently, the notion of phase synchronization has been extended to chaotic systems. We find that two weakly-coupled chaotic systems can be perfectly phase locked and their amplitudes are irrelevant. The definition of the phase of a chaotic system is not unique. Indeed, various versions have been proposed based on analytic signal processing methods [44] or the Poincaré section. Here, we use the former to study the phase synchronization of chaotic cavities. To obtain the temporal phase, observed in an arbitrary-scale time function  $s(t)$ , a complex analytic signal  $\phi(t)$  is reconstructed from

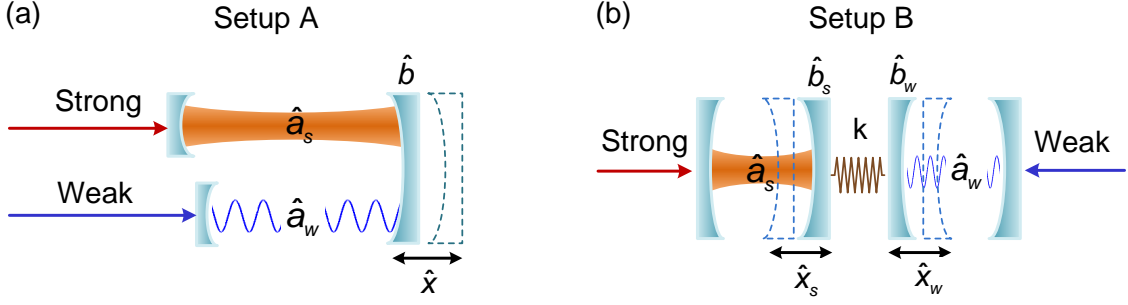


FIG. 2. (Color online) Schematic diagrams of two different setups for phase synchronization. (a) Setup A consists of a strongly-driven optical mode  $\hat{a}_s$ , a weakly-driven optical mode  $\hat{a}_w$ , and a mechanical mode  $\hat{b}$ . Both the optical modes are coupled to the mechanical resonator and integrated into a single optomechanical system; (b) Setup B includes one strongly-driven ( $\hat{a}_s$  and  $\hat{b}_s$ ) and one weakly-driven ( $\hat{a}_w$  and  $\hat{b}_w$ ) optomechanical systems, which are coupled via the mechanical modes  $\hat{b}_s$  and  $\hat{b}_w$  with a coupling coefficient  $k$ .

$s(t)$ , i.e.,

$$\phi(t) = s(t) + i\tilde{s}(t) = A(t) \exp[i\Psi(t)], \quad (12)$$

where  $A(t)$  is the amplitude of the signal and  $\Psi(t)$  is its phase, while  $\tilde{s}(t)$  is the Hilbert transform of  $s(t)$ , which is given by

$$\tilde{s}(t) = \frac{1}{\pi} \text{P.V.} \int_{-\infty}^{\infty} \frac{s(\tau)}{t - \tau} d\tau, \quad (13)$$

where P.V. denotes the Cauchy principal value. Note that the phases are unwrapped, i.e., these are not constrained to the range  $(-\pi, \pi)$ . Once  $s(t)$  is obtained, the amplitude  $A(t)$  and phase  $\Psi(t)$  can be calculated [44].

In this section, we describe a configuration for phase synchronization of a strongly-driven cavity mode and a weakly-driven one in an optomechanical system. To do so, we propose two setups, as shown in Figs. 2(a) and 2(b). Both setups consist of one strongly-driven mode, one weakly-driven cavity mode, and one or more mechanical mode(s). As mentioned in Sec. II, chaos can be generated in the strongly-driven cavity mode and be transferred to the weakly-driven cavity modes in mediation of the mechanical oscillation. When the driving-enhanced optomechanical coupling is strong and the cavity-driving detuning is small, i.e., in the strong optical-mechanical coupling and small-detuning regime, the temporal phase of each optical mode mainly depends on the displacement(s) of the mechanical resonator(s). In this configuration, the two chaotic optical cavity modes can be prepared in phase synchronization, regardless of their amplitudes. As in complete synchronization, here we also neglect thermal noise and quantum noise.

The detailed description of these two setups is presented in the following subsections.

#### A. Phase synchronization in setup A

As shown in Fig. 2(a), the system consists of a strongly-driven cavity mode  $\hat{a}_s$  and a weakly-driven cavity mode  $\hat{a}_w$ , and a mechanical mode  $\hat{b}$  associated with displacement  $\hat{x} =$

$x_{\text{ZPF}}(\hat{b}^\dagger + \hat{b})$ . These two cavity modes  $\hat{a}_s$  and  $\hat{a}_w$  are coupled to the mechanical mode  $\hat{b}$  in the unidirectional-coupling regime. Next we show how the phases of the two chaotic optical modes in the strongly- and weakly-driven regimes in setup A can be locked at a fixed ratio.

The total Hamiltonian of this system is described by

$$\begin{aligned} \hat{H} = & \Delta_s \hat{a}_s^\dagger \hat{a}_s + \Delta_w \hat{a}_w^\dagger \hat{a}_w + \Omega_m \hat{b}^\dagger \hat{b} \\ & + g_s \hat{a}_s^\dagger \hat{a}_s (\hat{b} + \hat{b}^\dagger) + i\varepsilon_s (\hat{a}_s^\dagger - \hat{a}_s) \\ & + g_w \hat{a}_w^\dagger \hat{a}_w (\hat{b} + \hat{b}^\dagger) + i\varepsilon_w (\hat{a}_w^\dagger - \hat{a}_w), \end{aligned} \quad (14)$$

where  $\Delta_s = \omega_{\text{cav},s} - \omega_{d,s}$  ( $\Delta_w = \omega_{\text{cav},w} - \omega_{d,w}$ ) is the corresponding detuning between the cavity resonance frequency  $\omega_{\text{cav},s}$  ( $\omega_{\text{cav},w}$ ) and the laser frequency  $\omega_{d,s}$  ( $\omega_{d,w}$ ), while  $\varepsilon_s$  ( $\varepsilon_w$ ) is the driving strength for the strongly (weakly) driven cavity mode, and  $\Omega_m$  is the resonance frequency of the mechanical resonator  $b$ . Here,  $g_s$  ( $g_w$ ) is the optomechanical single-photon coupling strength between the cavity mode  $\hat{a}_s$  ( $\hat{a}_w$ ) and the mechanical mode  $\hat{b}$ . For the Hamiltonian given in Eq. (14), we have the following quantum Langevin equations:

$$\dot{\hat{a}}_s = -i\Delta_s \hat{a}_s - \frac{\gamma_s}{2} \hat{a}_s - ig_s \hat{a}_s (\hat{b}^\dagger + \hat{b}) + \varepsilon_s, \quad (15a)$$

$$\dot{\hat{b}} = -i\Omega_m \hat{b} - \frac{\Gamma_m}{2} \hat{b} - ig_s \hat{a}_s^\dagger \hat{a}_s - ig_w \hat{a}_w^\dagger \hat{a}_w, \quad (15b)$$

$$\dot{\hat{a}}_w = -i\Delta_w \hat{a}_w - \frac{\gamma_w}{2} \hat{a}_w - ig_w \hat{a}_w (\hat{b}^\dagger + \hat{b}) + \varepsilon_w, \quad (15c)$$

where  $\gamma_s$  ( $\gamma_w$ ) and  $\Gamma_m$  are the damping rates of the cavity modes  $\hat{a}_s$  ( $\hat{a}_w$ ) and the mechanical mode  $\hat{b}$ , respectively. Let  $\alpha_s$ ,  $\alpha_w$ , and  $\beta$  be the mean values of  $\hat{a}_s$ ,  $\hat{a}_w$ , and  $\hat{b}$ :  $\alpha_s = \langle \hat{a}_s \rangle$ ,  $\alpha_w = \langle \hat{a}_w \rangle$ , and  $\beta = \langle \hat{b} \rangle$  in the classical regime. Their dynamics is governed by:

$$\dot{\alpha}_s = -i\Delta_s \alpha_s - \frac{\gamma_s}{2} \alpha_s - iG_s \alpha_s x + \varepsilon_s, \quad (16a)$$

$$\dot{\alpha}_w = -i\Delta_w \alpha_w - \frac{\gamma_w}{2} \alpha_w - iG_w \alpha_w x + \varepsilon_w, \quad (16b)$$

where  $G_s = g_s/x_{\text{ZPF}}^s$  ( $G_w = g_w/x_{\text{ZPF}}^w$ ) represents the coupling strength between the strongly (weakly) driven cavity mode  $\alpha_s$  ( $\alpha_w$ ) and the mechanical mode  $\hat{b}$ . The cavity modes  $\alpha_s$  and  $\alpha_w$

are two parts to be synchronized. They are driven by the same mechanical mode  $\beta$ . The mechanical motion is governed by

$$m_{\text{eff}}\ddot{x} = -m_{\text{eff}}\Omega_m^2 x - m_{\text{eff}}\Gamma_m \dot{x} + \hbar G_s |\alpha_s|^2, \quad (17)$$

where  $\Omega_m$  denotes the detuning of the mechanical mode  $\hat{b}$  and  $\gamma_m$  is its damping rate. In our arrangement, the effects of the weakly-driven optical modes acting on the mechanical mode  $x$  can be neglected by choosing  $G_s |\alpha_s|^2 \gg G_w |\alpha_w|^2$ .

Next, we find the relation of parameters determining the ratio of the unwrapped phase of cavity modes in phase synchronization. We define the mean value of the mechanical displacement  $x$  as  $\bar{x} = \lim_{t \rightarrow \infty} (t - t_0)^{-1} \int_{t_0}^t |x(t')| dt'$ , where  $t_0$  is the initial time. We refer to the conditions  $G_s \bar{x} \gg \Delta_s$  ( $G_w \bar{x} \gg \Delta_w$ ) and  $G_s \bar{x} \gg \gamma_s$  ( $G_w \bar{x} \gg \gamma_w$ ) as the strong-coupling small-detuning regime. In this regime, the instantaneous frequencies of both strong- and weakly-driven optical modes are determined by the following two factors: the detuning  $\Delta_s$  ( $\Delta_w$ ) and the mechanical displacement-dependent parameter  $G_s x$  ( $G_w x$ ). For on-resonance drivings,  $\Delta_s = \Delta_w \approx 0$ , the evolution of the strongly (weakly) driven optical mode  $\alpha_s$  ( $\alpha_w$ ) depends mainly on the mechanical motion  $G_s \bar{x}$  ( $G_w \bar{x}$ ). Thus, the unwrapped phases,  $\Psi_w(t)$  and  $\Psi_s(t)$  of the cavity modes  $\alpha_s$  and  $\alpha_w$ , defined in Eq. (12) are locked at a fixed ratio of

$$\lim_{t \rightarrow \infty} \frac{\Psi_w(t)}{\Psi_s(t)} = \frac{G_w}{G_s}, \quad (18)$$

as the time approaches infinity.

## B. Phase synchronization in setup B

As shown in Fig. 2(b), the setup B consists of a strongly-driven optomechanical system and a weakly-driven one, each of which includes only a single cavity mode and a mechanical mode. Different from setup A, two optomechanical resonators are mechanically coupled with each other with a coupling coefficient  $k$ . The total Hamiltonian of this synchronized system is

$$\begin{aligned} \hat{H} = & \Delta_s \hat{a}_s^\dagger \hat{a}_s + \Delta_w \hat{a}_w^\dagger \hat{a}_w + \Omega_s \hat{b}_s^\dagger \hat{b}_s + \Omega_w \hat{b}_w^\dagger \hat{b}_w \\ & + g_s \hat{a}_s^\dagger \hat{a}_s (\hat{b}_s + \hat{b}_s^\dagger) + g_w \hat{a}_w^\dagger \hat{a}_w (\hat{b}_w + \hat{b}_w^\dagger) \\ & + k (\hat{b}_w^\dagger + \hat{b}_w) (\hat{b}_s + \hat{b}_s^\dagger) + i \varepsilon_s (\hat{a}_s^\dagger - \hat{a}_s) \\ & + i \varepsilon_w (\hat{a}_w^\dagger - \hat{a}_w), \end{aligned}$$

where  $\hat{a}_s$  ( $\hat{a}_w$ ) denotes the annihilation operator of the strongly-driven (weakly-driven) cavity mode,  $\Delta_s$  ( $\Delta_w$ ) and  $\varepsilon_s$  ( $\varepsilon_w$ ) are the corresponding detuning and driving strengths. Here,  $\hat{b}_s$  ( $\hat{b}_w$ ) refers to the annihilation operators of the mechanical modes in the strongly (weakly) driven optomechanical system and  $\Omega_s$  ( $\Omega_w$ ) denotes its resonance frequency. Each cavity mode  $\hat{a}_s$  ( $\hat{a}_w$ ) is coupled to the mechanical mode  $\hat{b}_s$  ( $\hat{b}_w$ ) with the coupling strength  $g_s$  ( $g_w$ ), while  $k$  is the coupling strength between mechanical modes  $\hat{b}_w$  and  $\hat{b}_s$ . From the Hamiltonian of Eq. (19), we obtain the following quantum

Langevin equations:

$$\dot{\hat{a}}_s = -i\Delta_s \hat{a}_s - \frac{\gamma_s}{2} \hat{a}_s - i g_s \hat{a}_s (\hat{b}_s^\dagger + \hat{b}_s) + \varepsilon_s, \quad (19a)$$

$$\dot{\hat{b}}_s = -i\Omega_s \hat{b}_s - \frac{\Gamma_s}{2} \hat{b}_s - i g_s \hat{a}_s^\dagger \hat{a}_s, \quad (19b)$$

$$\dot{\hat{a}}_w = -i\Delta_w \hat{a}_w - \frac{\gamma_w}{2} \hat{a}_w - i g_w \hat{a}_w (\hat{b}_w^\dagger + \hat{b}_w) + \varepsilon_w, \quad (19c)$$

$$\dot{\hat{b}}_w = -i\Omega_w \hat{b}_w - \frac{\Gamma_w}{2} \hat{b}_w - i g_w \hat{a}_w^\dagger \hat{a}_w + i k (\hat{b}_s + \hat{b}_s^\dagger), \quad (19d)$$

where  $\gamma_s$  ( $\gamma_w$ ) and  $\Gamma_s$  ( $\Gamma_w$ ) denote the corresponding damping rates of the optical mode  $\hat{a}_s$  ( $\hat{a}_w$ ) and the mechanical mode  $\hat{b}_s$  ( $\hat{b}_w$ ) in the strongly (weakly) driven optomechanical system. Treating the whole system classically, we can replace operators with their mean values:  $\alpha_s = \langle \hat{a}_s \rangle$ ,  $\alpha_w = \langle \hat{a}_w \rangle$ ,  $\beta_s = \langle \hat{b}_s \rangle$ , and  $\beta_w = \langle \hat{b}_w \rangle$ . The dynamics of the weakly-driven optomechanical resonator is described by:

$$\dot{\alpha}_w = -i\Delta_w \alpha_w - \frac{\gamma_w}{2} \alpha_w + i G_w \alpha_w x_w + \varepsilon_w, \quad (20a)$$

$$m_w \ddot{x}_w = -m_w \Omega_w^2 x_w - m_w \Gamma_w \dot{x}_w + \hbar G_w |\alpha_w|^2 - K(x_w - x_s). \quad (20b)$$

In the unidirectional coupling regime, the motion of the weakly-driven optomechanical part is governed by the strongly-driven optomechanical one. The motion of the latter can be modeled as

$$\dot{\alpha}_s = -i\Delta_s \alpha_s - \frac{\gamma_s}{2} \alpha_s - i G_s \alpha_s x_s + \varepsilon_s, \quad (21a)$$

$$m_s \ddot{x}_s = -m_s \Omega_s^2 x_s - m_s \Gamma_s \dot{x}_s + \hbar G_s |\alpha_s|^2, \quad (21b)$$

where  $G_s = g_s/x_{\text{ZPF}}^s$  ( $G_w = g_w/x_{\text{ZPF}}^w$ ) is the optical-mechanical coupling strength in the strongly (weakly) driven optomechanical part. The displacements of the strongly- and weakly-driven mechanical oscillators are given by  $x_s = x_{\text{ZPF}}^s (\beta_s + \beta_s^*)$  and  $x_w = x_{\text{ZPF}}^w (\beta_w + \beta_w^*)$ , where  $x_{\text{ZPF}}^s$  and  $x_{\text{ZPF}}^w$  are the corresponding ZPF displacements of the left and right mechanical resonators, and  $m_s$  ( $m_w$ ) denotes the effective mass of the mechanical resonator  $b_s$  ( $b_w$ ). Here,  $-K(x_w - x_s)$  with a mechanical coupling strength  $K = \hbar k / (x_{\text{ZPF}}^s x_{\text{ZPF}}^w)$  is the external force driving the mechanical mode  $x_w$ . It provides a positive feedback to the weakly-driven mechanical mode  $x_w$  when  $(x_w - x_s) < 0$ . This feedback turns to be negative when  $(x_w - x_s) > 0$ . Thus, when the coupling coefficient  $k$  is strong enough, we have the relation:  $x_w(t) \approx x_s(t)$ . We define the mean value of the mechanical displacement  $x_m$  as  $\bar{x}_m = \lim_{t \rightarrow \infty} (t - t_0)^{-1} \int_{t_0}^t |x_m(t')| dt'$ , where  $t_0$  is the initial time and  $m = s$  ( $w$ ) stands for the strongly (weakly) driven mode. In the strong-coupling small-detuning regime when  $G_s \bar{x}_s \gg \Delta_s$  ( $G_w \bar{x}_w \gg \Delta_w$ ) and  $G_s \bar{x}_s \gg \gamma_s$  ( $G_w \bar{x}_w \gg \gamma_w$ ), the temporal phase of the strongly (weakly) driven optical mode  $\alpha_s$  ( $\alpha_w$ ) mainly depends on  $G_s \bar{x}_s$  ( $G_w \bar{x}_s$ ). Under these approximations, the ratio of the unwrapped phases  $\Psi_w(t)$  and  $\Psi_s(t)$  of  $\alpha_s$  and  $\alpha_w$  for this setup B in the infinite-time limit is the same as the corresponding limit, given in Eq. (18), for setup A.

We discuss our idea for the chaotic synchronization of optomechanical systems in the unidirectional coupling regime.

This treatment is reasonable as long as  $G_s|\alpha_s|^2 \gg G_w|\alpha_w|^2$ . It is worth noting that both complete and phase synchronization can be obtained with slight change in the chaotic motion of the mechanical resonators when the weak force from the weakly driven cavity modes on the mechanical resonators is taken into account.

## IV. RESULTS

In Sec. II, we presented four setups for both complete and phase synchronization of chaotic optical modes in an optomechanical system. These setups are different in their configurations but share a common dynamics: the strongly-driven cavity mode overwhelms the weakly-driven cavity modes and drives them into chaotic motion. Now we present our numerical results below for the configurations of these two types of synchronization.

### A. Complete synchronization

As mentioned above, we propose two setups for realizing complete synchronization. In both setups, the two weakly-driven cavity modes are controlled by the strongly-driven cavity mode. The complete synchronization of our setups is described by the APD model. The strongly-driven optical mode plays two key roles: (i) generating chaos and transferring it to the weakly-driven optical modes, mediated by the mechanical mode(s) and (ii) acting as a common external force on the weakly-driven optical modes.

#### 1. Complete synchronization in setup A

In setup A, the system consists of three cavity modes (i.e., one strongly-driven and two weakly-driven modes) and a mechanical mode. Each cavity mode is coupled to each other via the mechanical mode. To realize chaotic synchronization, first, we need to prepare the weakly-driven cavity modes  $\alpha_1$  and  $\alpha_2$  in chaotic states. However, in general, weakly-driven optomechanical systems can only generate nonchaotic fields. An efficient method to obtain a weak chaotic field is that connecting a weakly-driven cavity mode to a chaotic resonator. In this setup, chaos is generated by the strongly-driven cavity mode, and then transferred to the weakly-driven cavity modes  $\alpha_1$  and  $\alpha_2$  via the mechanical mode [21]. Here, the cavity mode  $\alpha_1$  is taken as an example to show how its dynamics transfers from regular into chaotic. To give a straightforward view of this transfer, we numerically calculate its phase portraits without [see Fig. 3(a)] and with [see Fig. 3(b)] the driving from the strongly-driven optical mode. Moreover, we calculate the largest Lyapunov exponent (LLE) of the system with the method proposed in [45, 46] to check if  $\alpha_1$  evolved to

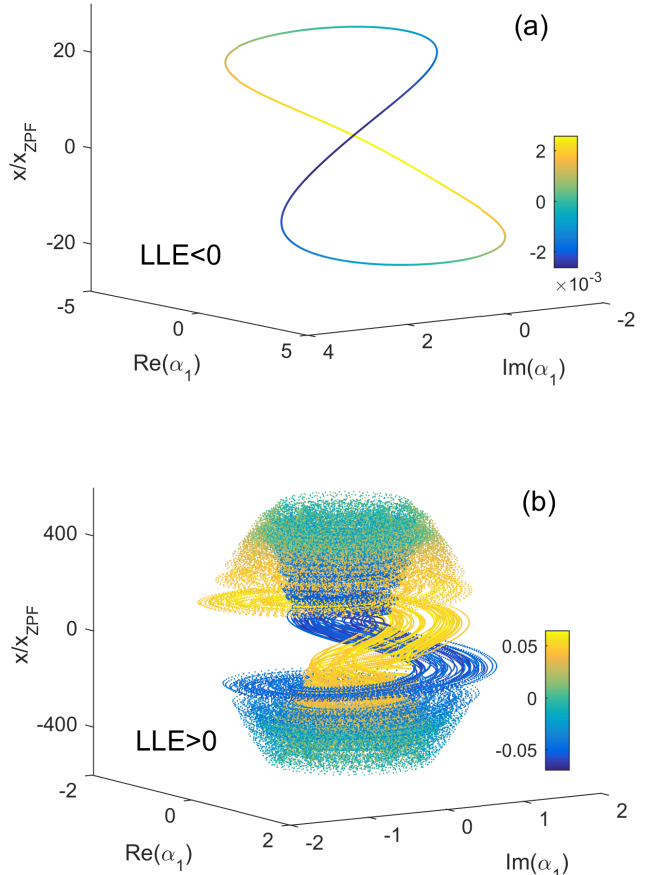


FIG. 3. (Color online) Complete synchronization in setup A: The phase portraits of optical cavity mode  $\alpha_1$  and the mechanical mode  $b$  (a) without and (b) with coupling to the strongly-driven cavity mode  $\alpha_s$ . The largest Lyapunov exponent (LLE) is calculated to be negative for case (a) and positive for case (b). Here,  $\text{Re}(\alpha_1)$ ,  $\text{Im}(\alpha_1)$ , and  $x$  correspond to the three coordinates of the three-dimensional phase space, and the fourth variable  $p$  in (a) and (b) is characterized in the color scale according to the depicted colorbar. The parameters are set as:  $\Delta_1/2\pi = 13$  MHz,  $\gamma_1/2\pi = \gamma_s/2\pi = 0.24$  GHz,  $g_1/2\pi = g_s/2\pi = 0.126$  GHz,  $\varepsilon_1/2\pi = 22$  MHz,  $\Delta_s/2\pi = 0.13$  GHz,  $\varepsilon_s/2\pi = 15.4$  GHz,  $\Gamma_m/2\pi = 2.8$  MHz,  $m_{\text{eff}} = 0.11$  fg, and  $\Omega_m/2\pi = 0.346$  GHz.

a chaotic state. A positive LLE is an indicator of chaos, while a negative LLE means regular motion.

We first consider the case of the absence of the cavity mode  $\alpha_s$ . In this case, the optomechanical system is reduced to a single weakly-driven optical mode  $\alpha_1$  and a single mechanical mode  $\beta_1$ . As shown in Fig. 3(a), a single closed loop is found in the phase portrait with  $\text{LLE} < 0$ , implying that the system is in regular periodic motion in the weakly-driven regime. Then, we study the system shown in Fig. 1(a), in which the two weakly-driven cavity modes are coupled to the strongly-driven cavity mode via the mechanical mode. It can be seen from the phase portrait that a chaotic attractor appears even if it is weakly driven [see Fig. 3(b)]. We find that  $\text{LLE} > 0$ . This means that the weakly-driven optical mode is

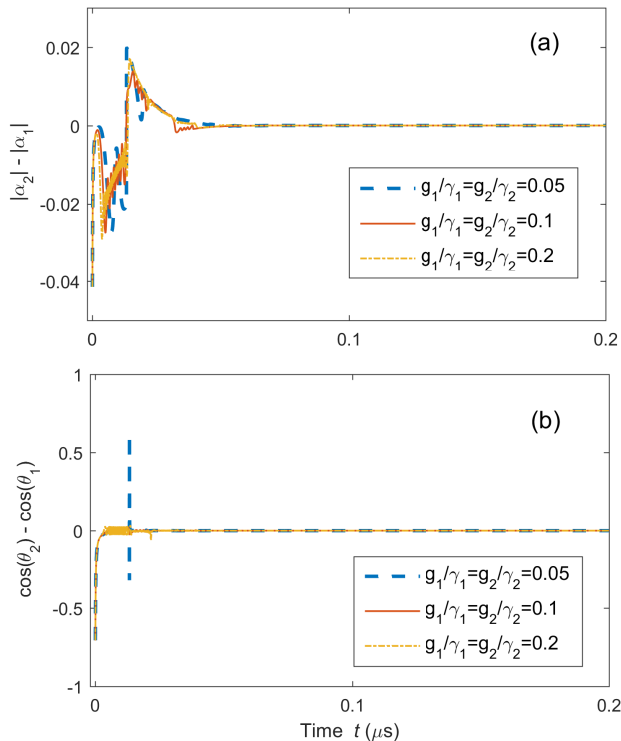


FIG. 4. (Color online) Synchronization errors for complete synchronization in setup A: (a) amplitude errors and (b) phase errors between the two chaotic weakly-driven cavity modes  $\alpha_1$  and  $\alpha_2$  as a function of time  $t$ . Here  $\Delta_2/2\pi = 13$  MHz,  $\gamma_2/2\pi = 0.24$  GHz, and  $\varepsilon_2/2\pi = 22$  MHz. The initial conditions are set as:  $\alpha_1(0) = 0.1 + 0.1i$ ,  $\alpha_2(0) = 0.1i$ ,  $\alpha_s(0) = 0$ , and  $\beta(0) = 0$ . All the other parameters are the same as in Fig. 3.

successfully driven to a chaotic state. The phase portraits in Fig. 3(b) consist of two complex variables: the weakly-driven cavity mode  $\alpha_1$  and the mechanical mode  $\beta$ . For simplicity, we expand this two-dimensional complex space  $(\alpha_1, \beta)$  to the four-dimensional real space  $[\text{Re}(\alpha_1), \text{Im}(\alpha_1), x, p]$ , where  $x$  and  $p$  denote the displacement and the momentum of the mechanical mode, respectively. The value of  $p$  is presented as different colors. In Fig. 3(b), we show that the weakly-driven cavity modes: (i) can be driven to the chaotic modes and (ii) can realize the synchronization with each other under the driving of the chaotic mechanical resonator.

We use the synchronization error between two chaotic fields  $\alpha_1$  and  $\alpha_2$  as the criterion of complete synchronization. The synchronization error includes the amplitude error  $|\alpha_2| - |\alpha_1|$  and phase error  $\cos\theta_2(t) - \cos\theta_1(t)$ , where  $|\alpha_1|$  ( $|\alpha_2|$ ) is the amplitude of the cavity mode  $\alpha_1$  ( $\alpha_2$ ), and its phase is denoted by  $\theta_1(t)$  [ $\theta_2(t)$ ]. The chaotic cavity fields  $\alpha_1$  and  $\alpha_2$  are completely synchronized if both of their amplitude and phase errors converge to zero as the evolution time progresses to infinity. Figure 4 shows the synchronization error between the two chaotic fields  $\alpha_1$  and  $\alpha_2$  for three different values of the coupling strengths  $g_1$  and  $g_2$ . Note that the initial conditions of  $\alpha_1$  and  $\alpha_2$  are set to be different. In gen-

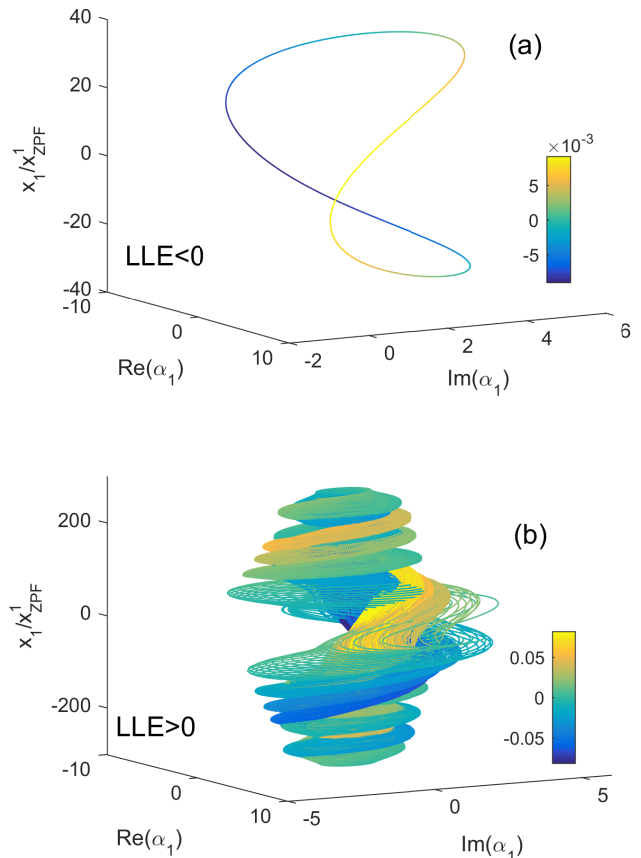


FIG. 5. (Color online) Complete synchronization in setup B: The phase portraits of an optomechanical system includes cavity 1 and the mechanical mode (a) without and (b) with coupling to the strongly-driven cavity mode. The largest Lyapunov exponent is calculated as: (a)  $\text{LLE} < 0$  and (b)  $\text{LLE} > 0$ . Here  $\text{Re}(\alpha_1)$ ,  $\text{Im}(\alpha_1)$ , and  $x_1$  correspond to the three coordinates of the three-dimensional phase space, and the fourth variable  $p_1$  in (a) and (b) are characterized by different colors shown according to the colorbars. The parameters are:  $\Delta_1/2\pi = 26$  MHz,  $g_1/2\pi = 25.2$  MHz,  $\Gamma_s/2\pi = \Gamma_1/2\pi = 2.8$  MHz,  $\Omega_s/2\pi = \Omega_1/2\pi = 0.346$  GHz, and  $k_1/2\pi = k_2/2\pi = 1.29$  MHz, while other parameters are the same as in Fig. 3.

eral, two neighboring chaotic trajectories without coupling will rapidly depart from each other because chaos is sensitive to initial conditions. However, we can find that both amplitude error  $|\alpha_2(t)| - |\alpha_1(t)|$  [see Fig. 4(a)] and phase error  $\cos\theta_2(t) - \cos\theta_1(t)$  [See Fig. 4(b)] decrease to zero after conquering the transient states. Thus, complete synchronization is obtained in the two weakly-driven cavity modes and this synchronization is independent of the coupling strengths  $g_1$  and  $g_2$ . Note that if the coupling strength  $g/\gamma_1 < 0.05$ , then the weakly-driven cavity mode  $\alpha_1$  cannot be driven to a chaotic state.

## 2. Complete synchronization in setup B



Now we study complete synchronization in setup B, shown in Fig. 1(b). The system includes three optomechanical subsystems: two weakly-driven optomechanical objects are coupled to the strongly-driven optomechanical one via the mechanical coupling. Here, the two optical modes  $\alpha_1$  and  $\alpha_2$  in two weakly-driven parts are chaotic and will be synchronized. In this subsection, we numerically show, by preparing the strongly-driven optomechanical part in a chaotic state, that the weakly-driven parts can also be driven into synchronized chaotic states.

Since the two weakly-driven components share the same dynamics, we choose one of them as an example to show the transfer from regular into chaotic motion. The phase portraits and the LLE of the weakly-driven optomechanical part  $(\alpha_1, \beta_1)$  are calculated for the cases without and with the strongly-driven optomechanical resonator. First, in the former case, a single loop is seen in the phase portrait shown in Fig. 5(a). This implies that the weakly-driven optomechanical part is in a periodic motion. This single loop becomes a chaotic attractor [see Fig. 5(b)] when the two weakly-driven optomechanical parts are coupled to the strongly-driven one. Moreover, this transition is also indicated by LLE, changing from negative in Fig. 5(a) to positive in Fig. 5(b). Similarly to Fig. 3, the complex two-dimensional weakly-driven optomechanical resonator  $[\alpha_1, \beta_1]$  is illustrated in the four-dimensional real space  $[\text{Re}(\alpha_1), \text{Im}(\alpha_1), x_1, p_1]$ . Here,  $\text{Re}(\alpha_1)$  [ $\text{Im}(\alpha_1)$ ] is the real (imaginary) part of the classical cavity mode  $\alpha_1$ , and  $x_1$  ( $p_1$ ) denotes the displacement (momentum) of the classical mechanical mode  $\beta_1$ . The color of the lines show the values of the fourth component  $p_1$ .

To answer the question whether the two chaotic cavity modes  $\alpha_1(t)$  and  $\alpha_2(t)$  can achieve complete synchronization, we calculate their error and check if it converges to zero. The error here includes the amplitude error  $|\alpha_2| - |\alpha_1|$  and the phase error  $\cos \theta_2(t) - \cos \theta_1(t)$ , where  $|\alpha_1|$  ( $|\alpha_2|$ ) and  $\cos \theta_1(t)$  [ $\cos \theta_2(t)$ ] denote the amplitude and phase of the cavity mode  $\alpha_1$  ( $\alpha_2$ ), respectively. Figures 6(a) and 6(b) show the amplitude and phase errors for different mechanical-coupling coefficients  $k_1$  and  $k_2$ . The initial condition difference is set to be:  $|\alpha_2| - |\alpha_1| = 0.0041$  in Fig. 6(a) and  $\cos \theta_2(t) - \cos \theta_1(t) = 1/\sqrt{2}$  in Fig. 6(b). When  $k_1$  and  $k_2$  are very weak ( $k_1/\gamma_1 = k_2/\gamma_2 = 10^{-4}$ ), both amplitude and phase errors considerably fluctuate [blue dashed curves in Figs. 6(a) and 6(b)] as the evolution time progresses. When  $k_1$  ( $k_2$ ) increases to  $k_1/\gamma_1 = k_2/\gamma_2 = 10^{-2}$  [green dashed dot curves in Fig. 6(a) and 6(b)], these two errors drastically fluctuate in the beginning, and then decrease to zero after conquering a transient period. Moreover, the increase of the coupling strength  $k_1$  ( $k_2$ ) accelerates the convergence of the synchronization errors, as shown in Figs. 6(a) and 6(b) (red solid curve). The time going to synchronization greatly decreases as the parameters  $k_1$  and  $k_2$  increase to  $k_1/\gamma_1 = k_2/\gamma_2 = 1$  from  $k_1/\gamma_1 = k_2/\gamma_2 = 10^{-2}$ . Obviously, the mechanical-coupling parameters  $k_1$  and  $k_2$  play a crucial role in the synchronization of chaotic optical fields. Two weakly-driven optomechanical systems can be driven into complete synchronization when the mechanical coupling  $k_1$  and  $k_2$  are

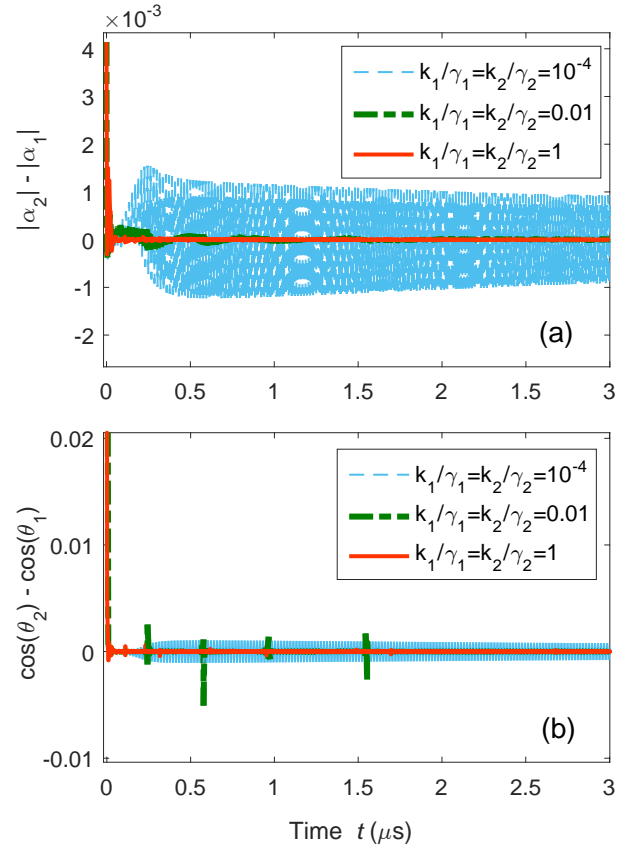


FIG. 6. (Color online) Synchronization errors for complete synchronization in setup B: (a) amplitude errors and (b) phase errors between the cavity modes  $\alpha_1$  and  $\alpha_2$  for different mechanical-mechanical coupling coefficients  $k_1$  and  $k_2$  as a function of time  $t$ . The initial conditions of the weakly- and strongly-driven optomechanical systems are set as:  $[\alpha_1(0), \beta_1(0)] = (0.01i, 0)$ ,  $[\alpha_2(0), \beta_2(0)] = (0.01 + 0.01i, 0)$ , and  $[\alpha_s(0), \beta_s(0)] = (0, 0)$ . The other parameters are the same as in Fig. 5.

large enough.

### 3. Comparison of setup A and setup B

Complete synchronization can be realized in both setups A and B according to the APD model. As shown in Figs. 4 and 6, the motions of the two weakly-driven cavity modes tend to be close to each other and become completely identical as the time progresses. As our theoretical prediction, the weakly-driven cavity modes in chaotic motion can be in complete synchronization if they are asymptotically stable and their motion is dominated by a common external force, which is the strongly-driven cavity mode here. Chaos can be transferred from the strongly-driven cavity mode to the weakly-driven cavity modes by mediation of a direct coupling in setup A (see Fig. 3) or indirect coupling in setup B (see Fig. 5). In setup A, the two weakly-driven cavity modes are synchronized. They are driven by the same mechanical mode.

Different from setup A, the action of the common external drive in setup B is indirectly applied to the two weakly-driven cavity modes via the mechanical coupling. The setup B highly relies on the mechanical coupling coefficient  $k_1$  and  $k_2$ . The motion of the optical modes of weakly-driven optomechanical systems is not only affected by its own oscillation but more crucially depends on the strongly-driven optomechanical one. When the mechanical-coupling coefficients are large, complete synchronization is achieved. However, for small  $k_1$  and  $k_2$ , the motion of the mechanical modes is dominated by the weakly driven optical modes. Thus, the external drive has little effect on the optical cavity modes to be synchronized. As a result, in the weak mechanical-coupling regime, complete synchronization is impossible in setup B.

## B. Phase synchronization

Phase synchronization is defined as the locking of the unwrapped phases in two dynamical systems. Below we will show phase synchronization of two chaotic optical modes in Fig. 2 in the strong-coupling small-detuning regime. Note that the unwrapped phases defined here are unfolded in every  $2\pi$ -period. This is essentially different from the phases introduced for complete synchronization in Sec. II.

### 1. Phase synchronization in setup A

In setup A, shown in Fig. 2(a), the weakly- and strongly-driven optical modes are coupled via a mechanical mode. When the cavity mode  $\hat{a}_s$  is strongly driven into a chaotic state, it, in turn, brings the mechanical mode into chaotic motion. As a result, the weakly-driven cavity mode is driven to a chaotic state via its coupling to the mechanical mode. The chaotic motion of two cavity modes is also proved by the positive LLE. In spite of being in chaotic motion, the motion trajectories of two chaotic optical modes have dramatically different amplitudes. However, two attractors rotate in a similar way with respect to the axis of  $\alpha_s = 0$  in Fig. 7(a) and  $\alpha_s = 0$  in Fig. 7(b), respectively. It indicates a correlation of the phases in the two attractors.

To study phase synchronization between the two chaotic optical modes, we calculate the ratio of the unwrapped phases of the strongly- and weakly-driven optical modes. To do so, we fix  $G_s$  but change the coupling strength  $G_w$  to see how the optomechanical coupling strength influences phase synchronization in the optomechanical system. The unwrapped phase  $\Psi_w(t)$  [ $\Psi_s(t)$ ] of the weakly (strongly) driven cavity mode is evaluated from the real part of the observed signal  $\text{Re}[\alpha_w(t)]$  ( $\text{Re}[\alpha_s(t)]$ ) with the analytic signal processing method. Phase synchronization occurs if the ratio of the phases of two non-identical optical modes can be locked at a fixed value of  $G_s/G_w$ , as  $t \rightarrow \infty$ , according to our discussion in Sec. II.

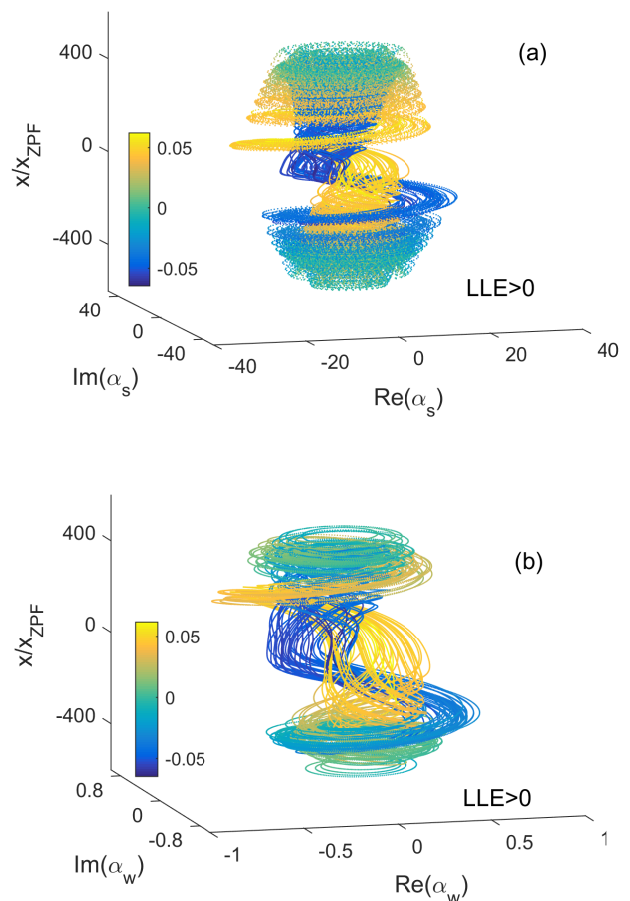


FIG. 7. (Color online) Phase synchronization in setup A: The phase portraits of (a) the strongly-driven and (b) weakly-driven optomechanical system. The largest Lyapunov exponent is positive in both cases. The parameters here are:  $\Delta_s/2\pi = 0.13$  GHz,  $\gamma_s/2\pi = 0.24$  GHz,  $g_s/2\pi = 0.126$  GHz,  $\varepsilon_s/2\pi = 15.4$  GHz,  $\Delta_w/2\pi = 26$  MHz,  $\gamma_w/2\pi = 52$  MHz,  $g_w/2\pi = 25.2$  MHz,  $\varepsilon_w/2\pi = 0.22$  GHz,  $\Gamma_m/2\pi = 2.8$  MHz, and  $\Omega_m/2\pi = 0.346$  GHz.

Figure 8 illustrates the evolutions of the ratio of unwrapped phase  $\Psi_s(t)/\Psi_w(t)$  as a function of the coupling strength  $G_w$ . When  $G_w$  is very weak, e.g.  $G_s/G_w = 100$ , the motion of the weakly-driven optical mode mainly depends on a given periodic input field. As a result, the ratio of  $\Psi_s(t)/\Psi_w(t)$  fluctuates over a large region [32, 34] and does not converge, see Fig. 8(a). When  $G_w$  is larger (e.g.  $G_s/G_w = 10$ ), [See Fig. 8(b)], the ratio of  $\Psi_s(t)/\Psi_w(t)$  fluctuates within a relative smaller region, but still cannot approach to a constant value [see Fig. 8(b)] because the influence of the input field and the driving of the mechanical mode on the weakly-driven optical mode compete with each other, leading to the randomly varying rhythms of the strongly- and weakly-driven cavity modes. In the strong-coupling regime, e.g.  $G_s/G_w = 1$ , the phase of the weakly-driven cavity mode is dominantly controlled by the chaotic mechanical mode. This mechanical mode also acts on the strongly-driven cavity mode simultaneously. In this case, the resonance frequencies of both the weakly- and strongly-driven cavity modes are determined by the motion of

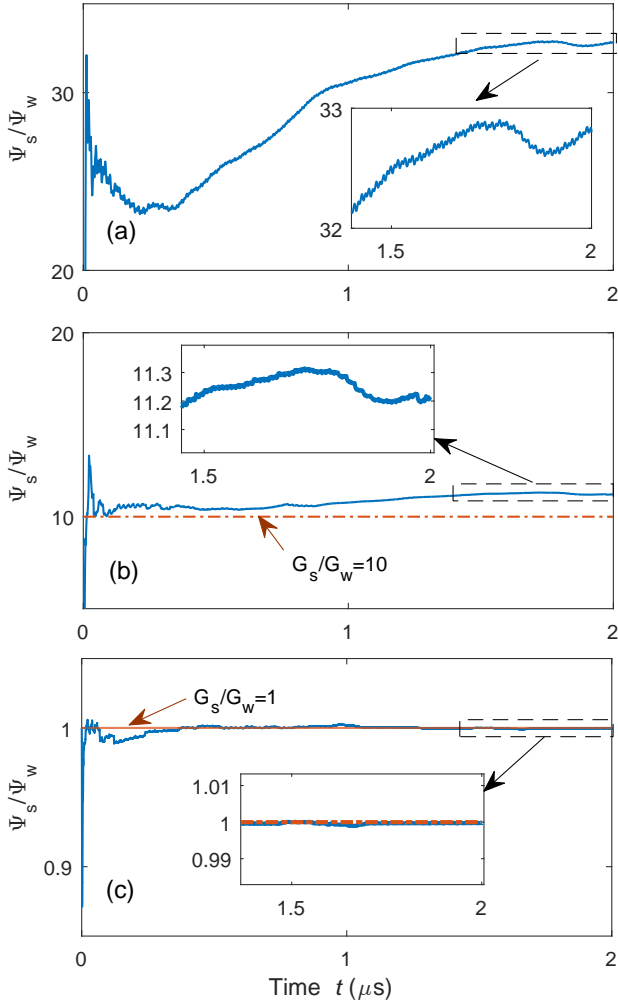


FIG. 8. (Color online) Phase synchronization in setup A: Evolutions of the ratios for the phases of the strongly-  $[\Psi_s(t)]$  and weakly-driven  $\Psi_w(t)$  cavity modes, when their coupling strengths are (a)  $G_s/G_w = 100$ , (b)  $G_s/G_w = 10$ , and (c)  $G_s/G_w = 1$ , where  $G_s = g_s/x_{ZPF}$  is a fixed value and  $G_w = g_w/x_{ZPF}$ . The red dashed line in each panel denotes the forecasting value  $G_s/G_w$ . Here,  $\varepsilon_w/2\pi = 1.1$  GHz,  $g_s = 0.126$  GHz, and the coupling strengths between the weakly-driven optical mode and the mechanical resonator are (a)  $g_w/2\pi = 1.26$  MHz, (b)  $g_w/2\pi = 12.6$  MHz, and (c)  $g_w/2\pi = 0.126$  GHz. The other parameters are the same as in Fig. 7.

the mechanical mode, see Fig. 8(c). The phase ratio converges to a constant value after oscillating over a transient period. These results show that phase synchronization can be realized in two chaotic optical oscillators, whereas their amplitudes are quite different. Moreover, the fixed value here approximately equals to the ratio of optomechanical strengths  $G_s/G_w = 1$  [red dashed line in Fig. 8(c)], consistent with our theoretical analysis.

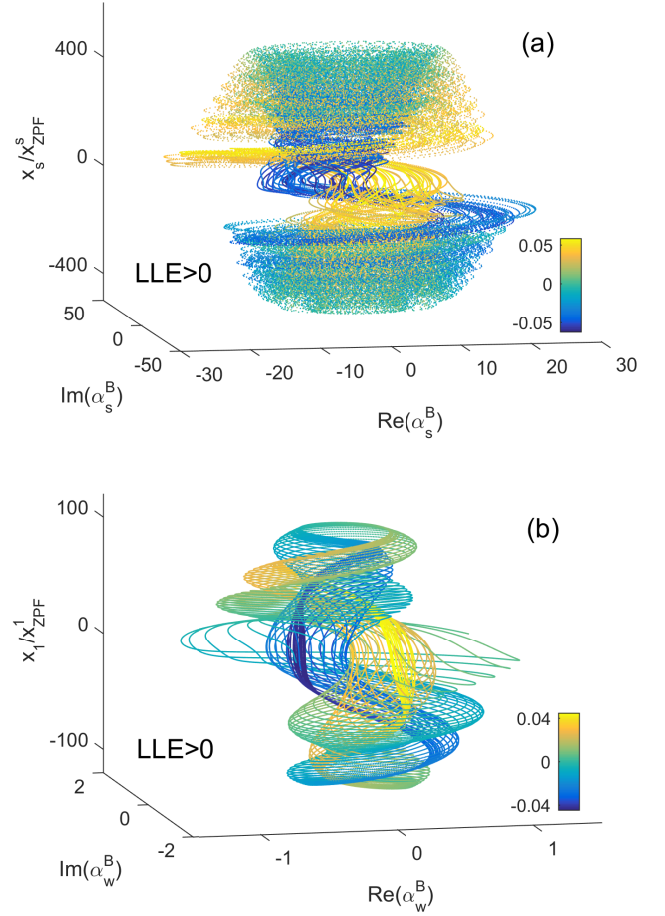


FIG. 9. (Color online) Phase synchronization in setup B: Phase portraits of (a) the strongly-driven and (b) the weakly-driven optomechanical systems. The largest Lyapunov exponent is positive in both cases. The parameters here are:  $\Gamma_s/2\pi = \Gamma_w/2\pi = 2.8$  MHz,  $\Omega_s/2\pi = \Omega_w/2\pi = 0.346$  GHz, and  $k/2\pi = 1.29$  MHz, while other parameters are the same as in Fig. 7.

## 2. Phase synchronization in setup B

In setup B shown in Fig. 2(b), the strongly- and weakly-driven optomechanical systems are coupled to each other with a rate  $k$  via the mechanical coupling between two mechanical oscillators. When  $k$  is strong enough, the motion of the weakly-driven optomechanical component (right-hand optomechanical resonator) is dominantly controlled by the strongly-driven optomechanical component (left-hand side one). Below, we will show, in the strong-coupling, small-detuning regime, the phases of the strongly- and weakly-driven cavity modes can be locked at a fixed ratio.

As an example, we take the set of values for parameters in Fig. 9 for the numerical simulation of the system motion with

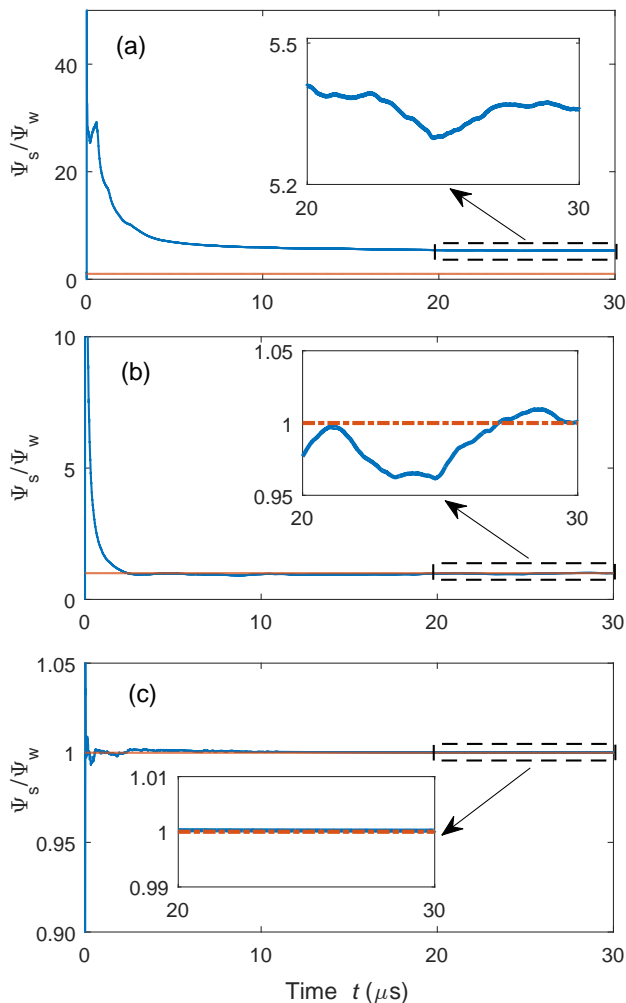


FIG. 10. (Color online) Phase synchronization in setup B: The ratios of the phases between the strongly- and weakly-driven optomechanical systems by varying the mechanical-coupling coefficient  $k$ : (a)  $k/\gamma_s = 10^{-3}$ , (b)  $k/\gamma_s = 10^{-2}$ , and (c)  $k/\gamma_s = 10^3$ . Here,  $g_s/2\pi = g_w/2\pi = 0.126$  GHz. All the other parameters are the same as in Fig. 9. The red line denotes the ratio of  $G_s/G_w$ .

Eqs. (22) and (23). As shown in Fig. 9(a), the phase portrait of the strongly-driven cavity mode shows a typical chaotic attractor and its LLE is positive. This chaotic cavity mode drives the mechanical oscillator,  $x_s$ , into chaotic motion. Due to the strong mechanical coupling between  $x_s$  and  $x_w$ , the mechanical oscillator  $x_w$  and subsequently the associated cavity mode under a weak driving are brought into chaotic motion. The chaotic motion of the weakly-driven optomechanical part can be seen in Fig. 9(b). The corresponding LLE is also positive, as an indicator of chaotic attractor.

To check if phase synchronization can be realized in setup B, we numerically calculate the time evolution of the unwrapped phases of the two cavity modes in the strongly- and weakly-driven optomechanical systems. Again, with the analytic signal processing method, we calculate the phases  $\Psi_w(t)$  and  $\Psi_s(t)$  from the optical signals  $\text{Re}[\alpha_w(t)]$  and  $\text{Re}[\alpha_s(t)]$  by

Eq. (12). Basically, the motion of the weakly-driven optomechanical part is determined by two factors: (i) its inherent oscillation and (ii) the driving of the strongly-driven optomechanical resonator. For the latter factor, the mechanical coupling coefficient  $k$  acts as the coupling strength between the strongly- and weakly-driven components. Here, we focus on the influence of  $k$  on phase synchronization.

Figure 10 shows the temporal evolution of the phase ratio,  $\Psi_w(t)/\Psi_s(t)$ , of two optical cavity modes for different mechanical-coupling strengths  $k$ . As mentioned above, in phase synchronization, the unwrapped phases of the two chaotic optical cavity modes should be locked at the value  $G_s/G_w$ , which refers to the coupling strength of the strongly-driven optomechanical part. To study the influence of the mechanical coupling on the phase synchronization, we set  $G_s/G_w = 1$  here. When  $k$  is very small ( $k/\gamma_s = 10^{-3}$ ), see Fig. 10(a), the motion of the weakly-driven optomechanical subsystem is separable from the strongly-driven one. As a result, its motion is mainly determined by itself. Thus, the phases of the two cavity modes in two parts are uncorrelated. The phase ratio  $\Psi_s(t)/\Psi_w(t)$  fluctuates in the range [5.2, 5.5] as the evolution time increases. As  $k/\gamma_s$  increases to  $10^{-2}$ , the ratio  $\Psi_s(t)/\Psi_w(t)$  oscillates around but cannot stay at the value  $G_s/G_w = 1$  as the evolution time progresses [see Fig. 10(b)]. In this case, the phase of the weakly-driven optomechanical system is mainly dependent on its own oscillation and the external driving force. It can be seen in the inset of Fig. 10(b) that  $\Psi_s(t)/\Psi_w(t)$  fluctuates in a much smaller range [0.95, 1.05], compared to the case in Fig. 10(a). When  $k/\gamma_s = 10^3$ , the motion of the weakly-driven cavity mode is governed by the strongly-driven optomechanical system. It leads to a perfect phase locking, as shown in Fig. 10(c). Note that there still exists a small discrepancy between  $\Psi_s(t)/\Psi_w(t)$  and  $G_s/G_w$ , mainly because the temporal phases of the optical cavity modes are also effected by its own oscillation. This phase mismatch decreases as the mechanical coupling coefficient  $k$  increases.

### 3. Comparison of setups A and B

Both setups A and B can be described as a common configuration in which the strongly-driven optical mode dominates the motion of the weakly-driven optical mode. To realize phase synchronization, setup A requires strong optomechanical coupling and weak detuning (the so-called strong-coupling small-detuning regime). Compared to setup A, the setup B additionally requires a strong coupling between the two mechanical resonators.

## V. CONCLUSIONS AND DISCUSSIONS

We have studied both complete and phase synchronization of optical cavity modes mediated by mechanical resonators. It is found that the complete synchronization of two identical optical cavity modes in chaotic motion can be obtained. We also showed the phase synchronization between two non-

identical optomechanical systems. In both types of chaotic synchronization, the chaotic displacement of the mechanical resonators is dominantly governed by the strongly-driven optical mode. The chaotic motion of the mechanical resonators subsequently pulls the weakly-driven optical cavity modes into chaotic motion. As a result, the phases of the strongly- and weakly-driven cavity modes can be synchronized. Our work provides a method to observe chaotic synchronization in experimentally-accessible optomechanical systems.

#### ACKNOWLEDGMENTS

The authors thank Yu-Xi Liu, Jing Zhang, Xuedong Hu, and Wei Qin for useful discussions. KX would like to

thank the National Key R&D Program of China (Grant No. 2017YFA0303703). AM and FN are partially supported by the MURI Center for Dynamic Magneto-Optics via the AFOSR Award No. FA9550-14-1-0040, the Japan Society for the Promotion of Science (KAKENHI), the IMPACT program of JST, CREST Grant No. JPMJCR1676, RIKEN-AIST Challenge Research Fund, JSPS-RFBR Grant No. 17-52-50023, and the Sir John Templeton Foundation.

- 
- [1] A. Pikovsky, M. Rosenblum, and J. Kurths, *Synchronization: a universal concept in nonlinear sciences* (Cambridge University Press, Cambridge, 2001).
- [2] S. Strogatz, *Sync: The emerging science of spontaneous order* (Penguin UK, London, 2004).
- [3] E. Ranta, V. Kaitala, and P. Lundberg, “A tale of big game and small bugs,” *Science* **285**, 1022 (1999).
- [4] K. Makino, Y. Hashimoto, J. Yoshikawa, H. Ohdan, T. Toyama, P. van Loock, and A. Furusawa, “Synchronization of optical photons for quantum information processing,” *Science Adv.* **2**, e1501772 (2016).
- [5] M. Morelli, C. C. J. Kuo, and M. O. Pun, “Synchronization techniques for orthogonal frequency division multiple access (OFDMA): A tutorial review,” *Proc. IEEE* **95**, 1394 (2007).
- [6] D. Antonio, D. H. Zanette, and D. Lopez, “Frequency stabilization in nonlinear micromechanical oscillators,” *Nat. Commun.* **3**, 806 (2012).
- [7] C. Hugenii, “Horoloquium oscillatorium,” *Apud F. Muguet* (1673).
- [8] T. Womelsdorf, J.-M. Schoffelen, R. Oostenveld, W. Singer, R. Desimone, A. K. Engel, and P. Fries, “Modulation of neuronal interactions through neuronal synchronization,” *Science* **316**, 1609 (2007).
- [9] J. Buck and E. Buck, “Mechanism of rhythmic synchronous flashing of fireflies,” *Science* **159**, 1319 (1968).
- [10] M. Toiya, H. O. Gonzalez-Ochoa, V. K. Vanag, S. Fraden, and I. R. Epstein, “Synchronization of chemical micro-oscillators,” *J. Phys. Chem. Lett.* **1**, 1241 (2010).
- [11] M. Aspelmeyer, T. J. Kippenberg, and F. Marquardt, “Cavity optomechanics,” *Rev. Mod. Phys.* **86**, 1391 (2014).
- [12] T. J. Kippenberg and K. J. Vahala, “Cavity opto-mechanics,” *Opt. Express* **15**, 17172 (2007).
- [13] W. Lechner, S. J. M. Habraken, N. Kiesel, M. Aspelmeyer, and P. Zoller, “Cavity optomechanics of levitated nanodumbbells: Nonequilibrium phases and self-assembly,” *Phys. Rev. Lett.* **110**, 143604 (2013).
- [14] Y.-C. Liu, Y.-F. Xiao, X. S. Luan, and C. W. Wong, “Dynamic dissipative cooling of a mechanical resonator in strong coupling optomechanics,” *Phys. Rev. Lett.* **110**, 153606 (2013).
- [15] M. Cirio, K. Debnath, N. Lambert, and F. Nori, “Amplified optomechanical transduction of virtual radiation pressure,” *Phys. Rev. Lett.* **119**, 053601 (2017).
- [16] F. Brennecke, S. Ritter, T. Donner, and T. Esslinger, “Cavity optomechanics with a Bose-Einstein condensate,” *Science* **322**, 235 (2008).
- [17] H. Jing, S. K. Özdemir, X.-Y. Lü, J. Zhang, L. Yang, and F. Nori, “ $\mathcal{PT}$ -symmetric phonon laser,” *Phys. Rev. Lett.* **113**, 053604 (2014).
- [18] X.-Y. Lü, H. Jing, J.-Y. Ma, and Y. Wu, “ $\mathcal{PT}$ -symmetry-breaking chaos in optomechanics,” *Phys. Rev. Lett.* **114**, 253601 (2015).
- [19] X. F. Jiang, L. B. Shao, S.-X. Zhang, X. Yi, J. Wiersig, Li Wang, Q. H. Gong, M. Loncar, L. Yang, and Y.-F. Xiao, “Chaos-assisted broadband momentum transformation in optical microresonators,” *Science* **358**, 344 (2017).
- [20] M. Sciamanna, “Vibrations copying optical chaos,” *Nat. Photon.* **10**, 366 (2016).
- [21] F. Monifi, J. Zhang, S. K. Özdemir, B. Peng, Y.-X. Liu, F. Bo, F. Nori, and L. Yang, “Optomechanically induced stochastic resonance and chaos transfer between optical fields,” *Nat. Photon.* **10**, 399 (2016).
- [22] D. Navarro-Urrios, N. E. Capuj, M. F. Colombano, P. D. García, M. Sledzinska, F. Alzina, A. Griol, A. Martinez, and C. M. Sotomayor-Torres, “Nonlinear dynamics and chaos in an optomechanical beam,” *Nat. Commun.* **8**, 14965 (2017).
- [23] L. Bakemeier, A. Alvermann, and H. Fehske, “Route to chaos in optomechanics,” *Phys. Rev. Lett.* **114**, 013601 (2015).
- [24] T. Carmon, M. C. Cross, and K. J. Vahala, “Chaotic quivering of micron-scaled on-chip resonators excited by centrifugal optical pressure,” *Phys. Rev. Lett.* **98**, 167203 (2007).
- [25] M. Zhang, G. S. Wiederhecker, S. Manipatruni, A. Barnard, P. McEuen, and M. Lipson, “Synchronization of micromechanical oscillators using light,” *Phys. Rev. Lett.* **109**, 233906 (2012).
- [26] M. Bagheri, M. Poot, L. Fan, F. Marquardt, and H. X. Tang, “Photonic cavity synchronization of nanomechanical oscillators,” *Phys. Rev. Lett.* **111**, 213902 (2013).
- [27] M. Zhang, S. Shah, J. Cardenas, and M. Lipson, “Synchronization and phase noise reduction in micromechanical oscillator arrays coupled through light,” *Phys. Rev. Lett.* **115**, 163902 (2015).
- [28] N. Lorch, E. Amitai, A. Nunnenkamp, and C. Bruder, “Genuine quantum signatures in synchronization of anharmonic self-oscillators,” *Phys. Rev. Lett.* **117**, 073601 (2016).

- [29] G. Heinrich, M. Ludwig, J. Qian, B. Kubala, and F. Marquardt, "Collective dynamics in optomechanical arrays," *Phys. Rev. Lett.* **107**, 043603 (2011).
- [30] M. Ludwig and F. Marquardt, "Quantum many-body dynamics in optomechanical arrays," *Phys. Rev. Lett.* **111**, 073603 (2013).
- [31] T. Weiss, A. Kronwald, and F. Marquardt, "Noise-induced transitions in optomechanical synchronization," *New J. Phys.* **18**, 013043 (2016).
- [32] T. Li, T.-Y. Bao, Y.-L. Zhang, C.-L. Zou, X.-B. Zou, and G.-C. Guo, "Long-distance synchronization of unidirectionally cascaded optomechanical systems," *Optics Express* **24**, 12336 (2016).
- [33] K. Shlomi, D. Yuvaraj, I. Baskin, O. Suchoi, R. Winik, and E. Buks, "Synchronization in an optomechanical cavity," *Phys. Rev. E* **91**, 032910 (2015).
- [34] E. Gil-Santos, M. Labousse, C. Baker, A. Goetschy, W. Hease, C. Gomez, A. Lemaitre, G. Leo, C. Ciuti, and I. Favero, "Light-mediated cascaded locking of multiple nano-optomechanical oscillators," *Phys. Rev. Lett.* **118**, 063605 (2017).
- [35] S. Boccaletti, J. Kurths, G. Osipov, D. L. Valladares, and C. S. Zhou, "The synchronization of chaotic systems," *Phys. Rep.* **366**, 1 (2002).
- [36] L. Kocarev and U. Parlitz, "General approach for chaotic synchronization with applications to communication," *Phys. Rev. Lett.* **74**, 5028 (1995).
- [37] U. Parlitz, L. Kocarev, T. Stojanovski, and H. Preckel, "Encoding messages using chaotic synchronization," *Phys. Rev. E* **53**, 4351 (1996).
- [38] L. M. Pecora and T. L. Carroll, "Synchronization in chaotic systems," *Phys. Rev. Lett.* **64**, 821 (1990).
- [39] M. G. Rosenblum, A. S. Pikovsky, and J. Kurths, "Phase synchronization of chaotic oscillators," *Phys. Rev. Lett.* **76**, 1804 (1996).
- [40] E. Rosa, E. Ott, and M. H. Hess, "Transition to phase synchronization of chaos," *Phys. Rev. Lett.* **80**, 1642 (1998).
- [41] N. F. Rulkov, M. M. Sushchik, L. S. Tsimring, and H. D. I. Abarbanel, "Generalized synchronization of chaos in directionally coupled chaotic systems," *Phys. Rev. E* **51**, 980 (1995).
- [42] L. Kocarev and U. Parlitz, "Generalized synchronization, predictability, and equivalence of unidirectionally coupled dynamical systems," *Phys. Rev. Lett.* **76**, 1816 (1996).
- [43] M. G. Rosenblum, A. S. Pikovsky, and J. Kurths, "From phase to lag synchronization in coupled chaotic oscillators," *Phys. Rev. Lett.* **78**, 4193 (1997).
- [44] A. J. E. M. Janssen, "Gabor representation of generalized functions," *J. Math. Anal. Appl.* **83**, 377 (1981).
- [45] A. Wolf, J. B. Swift, H. L. Swinney, and J. A. Vastano, "Determining Lyapunov exponents from a time series," *Physica D* **16**, 285 (1985).
- [46] K. Briggs, "An improved method for estimating Lyapunov exponents of chaotic time series," *Phys. Lett. A* **151**, 27 (1990).